J. CHEM. SOC. FARADAY TRANS., 1994, 90(4), 541–548

Kinetics of Thermal Decomposition of the Diazines: Shock-tube Pyrolysis of Pyrimidine

Alan Doughty and John C. Mackie*
Department of Physical and Theoretical Chemistry, University of Sydney, NSW 2006, Australia

The kinetics of pyrolysis of pyrimidine diluted in argon have been studied behind reflected shock waves over the temperature range 1200–1850 K, at uniform gas residence times of 850–1000 μs and pressures of 13–15 atm. The major products of pyrimidine pyrolysis were found to be acetylene, HCN, acrylonitrile, cyanoacetylene and H_2. Using both end-product analysis and real-time UV spectrometry the kinetics of pyrimidine disappearance were found to be first order with respect to reactant concentration over the concentration range of 0.07–0.3 mol%. The two techniques yielded a first-order rate constant (k_{dis}) for the disappearance of pyrimidine given by the expression $10^{12.3(\pm 0.4)} \exp[-275(\pm 13)\ \text{kJ mol}^{-1}/RT]\ \text{s}^{-1}$.

A detailed reaction model incorporating a free-radical mechanism for the decomposition of pyrimidine has been developed, and shown to predict the reactant and product concentrations between 1250 and 1600 K. Important radicals in the mechanism were found to be *o*- and *p*-pyrimidyl, with H atoms and CN radicals being radical chain carriers. Sensitivity and flux analysis of the kinetic model has shown the most important initiation pathway to be the loss of an H atom from pyrimidine to yield *o*-pyrimidyl. Optimisation of the Arrhenius parameters for this initiation reaction yields an activation energy consistent with a heat of formation of the *o*-pyrimidyl radical of $376(\pm 10)\ \text{kJ mol}^{-1}$.

This study of the pyrolysis of pyrimidine is part of a wider study aimed at investigating the mechanism by which oxides of nitrogen (NO_x) are formed from the combustion of coal and heavy fuels. Combustion of these materials, at least under fuel-rich conditions, is thought to proceed first by the thermal decomposition of the fuel, followed by reaction of the pyrolysis products with oxygen. Study of the pyrolysis of nitrogen-containing molecules present in coal should therefore contribute to the understanding of the mechanism of NO_x formation during coal combustion.

Gaining insight into the NO_x formation process by studying the pyrolysis of coal model compounds requires knowledge of the functional form of nitrogen in the unperturbed coal matrix. The pyrolysis of pyridine, pyrrole and 2-picoline have all been studied by this group.[1–4] These compounds were chosen as models on the basis of analysis of coal-derived liquids,[5] and on the results of X-ray photoelectron spectroscopy (XPS) studies[6,7,8] on coal, which indicated that the pyridine and pyrrole rings were important forms of nitrogen. It is possible, however, that the broadness of XPS peaks results in the significance of the diazines being underestimated. The DNA bases thymine and cytosine both are derivatives of pyrimidine, and their presence in plant and microbial DNA would be expected to lead to their presence in soils, and possibly coal. Pyrimidine has been found to be present in soils[9] and coal analysis has found that compounds containing two or more nitrogens are significant sources of nitrogen in coal.[10] Pyrimidine could therefore be considered to be a useful model compound for the study of the evolution of NO_x during coal combustion.

An important part of this study has been the development of a detailed kinetic reaction mechanism which can model the temperature profiles for product formation and of depletion of the reactant. The kinetic model consists of 25 reactions and 18 species, and successfully models the thermal decomposition of pyrimidine over the temperature range 1250 to 1600 K, at a pressure of 13–15 atm.

Experimental

Pyrolysis experiments were carried out using the single-pulse shock tube (SPST). On-line capillary and packed column gas chromatography (GC) were used to quantify the major and minor products. In addition to the analysis of end products, the kinetics of decomposition of pyrimidine was also probed using real-time UV spectrometry. Details of the shock tube,[11,12] GC analysis[3] and UV spectrometry[3] have been given elsewhere. In this study the GC analysis differs slightly from that previously described[3] in that all products, including nitrogen compounds, were quantified using a flame ionisation detector (FID).

Pyrimidine used in this study was obtained from Aldrich, of stated purity >98%. The pyrimidine was used without further purification to prepare mixtures of the vapour dilute in argon at concentrations of 0.2–0.4 mol%. Experiments were also carried out at a lower concentration range of 0.06–0.08 mol%. Analysis of the reactant mixtures by GC yielded >99.5% of the nitrogen present as pyrimidine.

Products were identified using gas chromatography–mass spectrometry (GC–MS) as described in ref. 3. Assignments were confirmed by comparison with commercial samples where available.

FID responses for pyrimidine and its decomposition products were measured using commercially available samples. In the case of cyanoacetylene the FID response was estimated assuming its response to be similar to acrylonitrile and ethylcyanide. The yield of cyanogen could not be quantified since a calibration sample was not available, and there is no other molecule which might be expected to possess a similar FID response.

End-product analysis for the low-concentration series of experiments can be considered to be less accurate than the end-product analysis performed for the higher concentration series. This is a consequence of the considerably lower concentrations of the species present in the product mixtures for the low-concentration series. This problem is exacerbated in the measurement of HCN due to the relatively low sensitivity of the FID to HCN. For example, the FID is more sensitive to pyrimidine compared to HCN by a factor of nine. This low sensitivity results in the measurement of HCN in the low-concentration series being less accurate than the measurements made for other products of pyrimidine decomposition, in the low-concentration series of experiments.

Hydrogen was measured using a previously described GC method.[3] The limit of detection for hydrogen was found to be

0.05 mol%. A measurement of 0.05 mol% hydrogen from an initial concentration of pyrimidine of 0.3 mol% would correspond to a yield (based on the original pyrimidine) of hydrogen of 17%. Therefore hydrogen measurements could only be made where the yield of hydrogen was greater than 17%. This was only observed at intermediate to high levels of decomposition. The relatively high limit of detection for hydrogen precluded the measurement of hydrogen for the low-concentration series.

Real-time UV spectrometry was carried out at two wavelengths, both corresponding to vibronic bands of the $^1B_1 \leftarrow {}^1A_1(\pi^* n)$ electronic transition of pyrimidine.[13] The majority of the UV kinetic data was obtained by monitoring the absorption at a wavelength corresponding to the 0–0 vibronic band of the above-mentioned electronic transition, which occurs at *ca.* 320.8 nm (using a 1 nm bandpass). No significant difference was observed when comparing data obtained at this wavelength with data obtained when monitoring absorption changes at 290 nm (2 nm bandpass).

The two techniques were used to obtain overall decomposition kinetics over the temperature range 1200–1850 K. End-product analysis allowed the decomposition products to be profiled over the temperature range 1250–1600 K, which corresponded to pyrimidine decomposition between 0 and 90%. Temperatures and pressures in the reflected shock were calculated from measured incident and reflected shock velocities. Residence times were in the range of 850–1000 μs, with reaction pressures of 13–15 atm.

Results

The major nitrogen-containing products for the decomposition of pyrimidine were HCN, acrylonitrile and cyanoacetylene. Temperature profiles for these products, and for the disappearance of the reactant are given in Fig. 1–5. Cyanogen was observed at what appeared to be low levels. Traces of pyrazine were also present in the reaction products at low extents of decomposition. The only major hydrocarbon product was found to be acetylene. At moderate to high extents of decomposition, methane, ethylene, vinylacetylene and diacetylene were minor hydrocarbon products. Hydrogen was found to be a major product, at intermediate to high extents of decomposition. The high limit of detection for hydrogen prevented the detection of hydrogen at low extents of pyrimidine decomposition.

Since much of the kinetic data in this study are in the form of temperature profiles of reactant and product concentrations, it is important to ascertain whether the concentrations

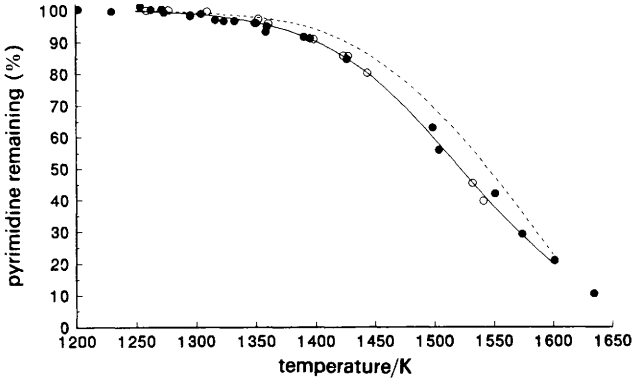

Fig. 1 Temperature dependence of % pyrimidine remaining in the pyrolysis of pyrimidine, with initial concentrations of pyrimidine of 0.2–0.4% (●) and 0.06–0.08 mol% (○) in Ar. Model predictions for 0.3 and 0.07 mol% pyrimidine in Ar, are represented by (——) and (– – –), respectively.

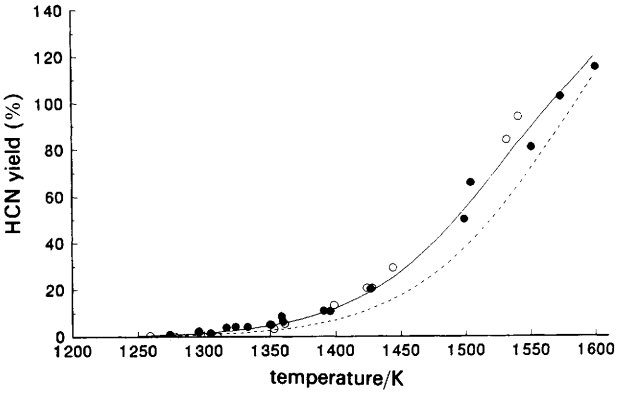

Fig. 2 Temperature dependence of the yield of HCN from pyrolysis of pyrimidine. Symbols as in Fig. 1.

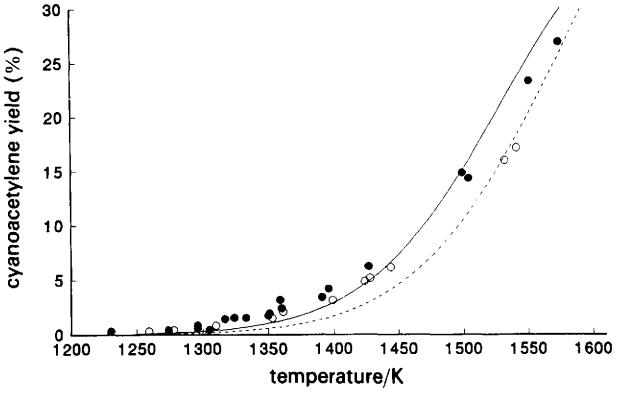

Fig. 3 Temperature dependence of the yield of cyanoacetylene from pyrolysis of pyrimidine. Symbols as in Fig. 1.

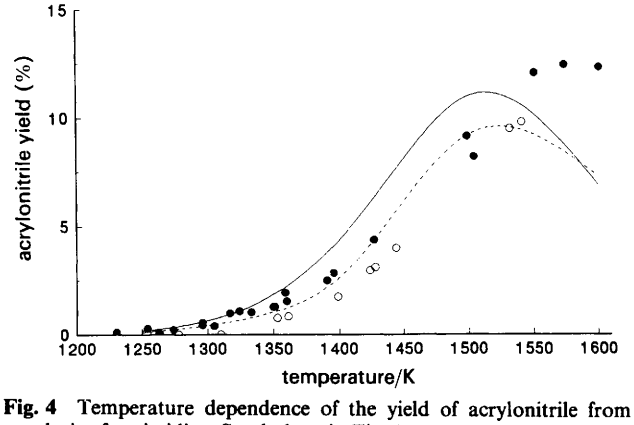

Fig. 4 Temperature dependence of the yield of acrylonitrile from pyrolysis of pyrimidine. Symbols as in Fig. 1.

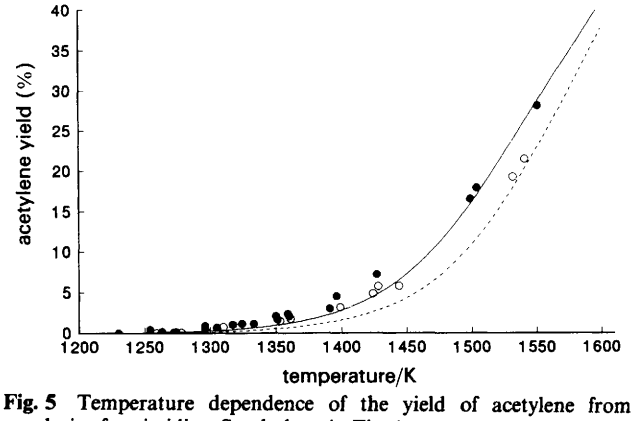

Fig. 5 Temperature dependence of the yield of acetylene from pyrolysis of pyrimidine. Symbols as in Fig. 1.

of species measured in the product gas mixtures are consistent with the concentration of pyrimidine prior to reaction. To ensure this consistency, and thus the validity of the data, mass balance calculations were performed for each run conducted. In Fig. 6, the N recovered in the post shock mixture (*i.e.* the sum of N in the products, including unreacted pyrimidine) is plotted as a percentage of the measured concentration of pyrimidine in the unreacted gas mixture. As can be seen from the plot, the bulk of the recovery data falls between 90 and 110%. The deviation at very high extents of pyrimidine decomposition is most likely due to limitations in the accuracy of the HCN calibration constant. The most important observation to make from the mass balance plot is that at low to moderate extents of decomposition there is no systematic loss of nitrogen from the system. This suggests that cyanogen could not be a major product of the decomposition of pyrimidine.

When the results from the runs carried out with the higher initial concentration of pyrimidine (0.2–0.4 mol%) are compared with the runs carried out at lower initial concentration (0.06–0.08 mol%), no significant differences in the reactant decomposition profile can be observed. This suggests that the decomposition of pyrimidine is close to first order with respect to the reactant concentration, under the conditions of this study.

The time-resolved UV signal intensities measured during the passage of the shock wave were used to calculate the absorbances (A) at the corresponding wavelength from the expression derived from the Beer–Lambert Law:

$$A = -\log(I/I_0)$$

where I is the photomultiplier output (V), and I_0 the photomultiplier output (V) at 100% transmittance.

A typical absorption trace as a function of time during the passage of a shock wave is included in Fig. 7. The change in absorption due to the increase in density at the arrival of the incident and reflected shock fronts can be clearly seen, followed by a decay due to the decomposition of the pyrimidine. The major products of the decomposition of pyrimidine do not absorb light at either of the wavelengths probed, so the absorption decay trace should be entirely due to the disappearance of the reactant. This is supported by the observation that the kinetics from measurements taken by monitoring the UV absorption at 290 nm showed no difference to the kinetics obtained from absorption measurements conducted at 320.8 nm. In view of the low concentrations of pyrimidine used in this study, the decrease in temperature due to reaction would be expected to be less than 2 K.

Since the absorbance in the reflected shock is proportional to the pyrimidine concentration, a first-order rate constant

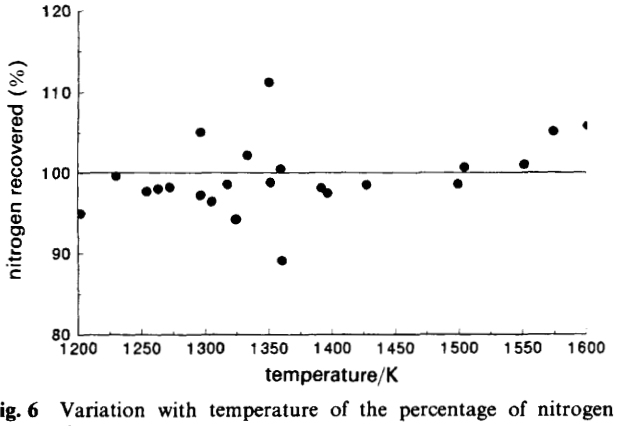

Fig. 6 Variation with temperature of the percentage of nitrogen recovered

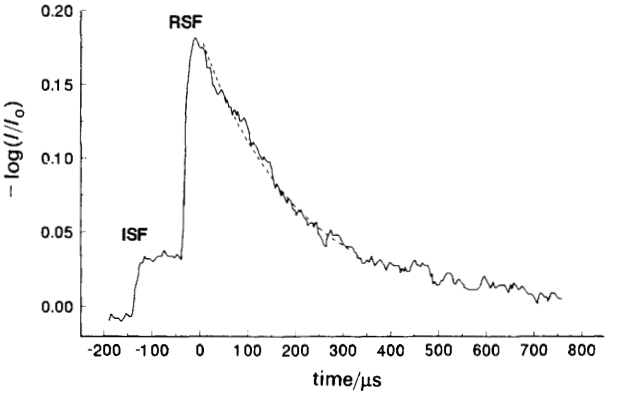

Fig. 7 Real-time absorbance trace of light of wavelength 320 nm in a shock wave heated mixture of 0.23 mol% pyrimidine in Ar (——). Least-squares fit of the exponential decay of the absorbance is also shown (– – –). Times are shown from $t = 0$ as used in the exponential fit. Reflected shock gas temperature, 1682 K. ISF = incident shock front, RSF = reflected shock front.

for the disappearance of pyrimidine can be calculated from the absorbance decay traces. Using the method of least squares, the absorbance decay was fitted to the expression:

$$A = b \exp(-k_{dis} t)$$

where t is the time from the arrival of the reflected shock front, b is a constant and k_{dis} is the first-order rate constant. The resulting exponential function is plotted in Fig. 7.

A first-order rate constant for pyrimidine disappearance can also be calculated from the SPST data. If the decomposition of pyrimidine is taken as being first order with respect to the reactant concentration, k_{dis} can be calculated from the following expression:

$$k_{dis} = (1/t_{res})\ln(y/100)$$

where t_{res} is the residence time of the reaction and y is the percentage of pyrimidine remaining in the product gases.

Calculations of k_{dis} from the UV-absorption measurements and the SPST data are summarised in the Arrhenius plot in Fig. 8. As can be seen from the plot, the two techniques for obtaining k_{dis} cover complementary temperature ranges. Values for k_{dis} calculated from SPST data are taken from measurements at low to moderate extents of decomposition, whereas UV spectroscopic measurements of k_{dis} are taken at temperatures where the pyrimidine has undergone moderate to complete decomposition at the end of the residence time.

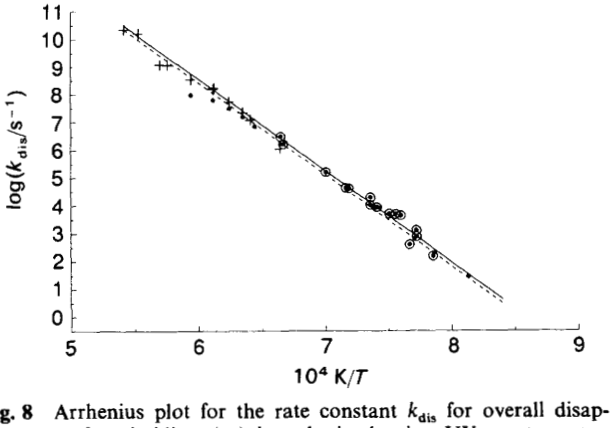

Fig. 8 Arrhenius plot for the rate constant k_{dis} for overall disappearance of pyrimidine. (+) k_{dis} obtained using UV spectrometry, (– – –) regression fit to UV spectrometric k_{dis}. (●) k_{dis} from end-product analysis, (——) regression fit to end-product k_{dis}. (○) k_{dis} values used in regression fit to end-product k_{dis}.

Table 1 Pseudo-Arrhenius parameters for the formation of the major products of pyrimidine decomposition

product	A/s^{-1}	E_a/kJ mol^{-1}
cyanoacetylene	11.4 (±1.3)	259 (±29)
HCN	12.6 (±1.0)	279 (±22)
acrylonitrile	10.9 (±0.8)	250 (±21)
acetylene	11.6 (±0.8)	266 (±19)

The linearity of the Arrhenius plots in Fig. 8 indicate that the Arrhenius pre-exponential factor for the decomposition of pyrimidine shows no discernible temperature dependence.

Arrhenius parameters for the disappearance of pyrimidine have been calculated from the Arrhenius plots using linear regression analysis. For the SPST data, and Arrhenius pre-exponential factor of $10^{12.3(\pm 0.5)}$ s^{-1} and an apparent activation energy of 275(±13) kJ mol^{-1} were obtained. This is in excellent agreement with the values taken from the UV spectrophotometric data, which yielded an Arrhenius pre-exponential factor of $10^{12.3(\pm 0.4)}$ s^{-1} and an apparent activation energy of 275(±13) kJ mol^{-1}.

Pseudo-Arrhenius parameters for the formation of the major products have also been calculated from the SPST data. The pseudo-first-order rate constants for the formation of these products (k_{form}) were calculated from the approximate expression:

$$k_{form} = c/(100t_{res})$$

where c is the concentration of the product (in yield %) in the product gas. This approximate expression is only valid at low extents of decomposition, and thus only data for the first 20% of pyrimidine decomposition are used in these calculations. Arrhenius parameters taken from the k_{form} data for each of the products are summarised in Table 1.

Discussion

The pyrolysis of pyrimidine yields four major products, all of which are present in concentrations which are not related to the concentrations of other products by any simple whole number ratio. This type of product distribution is consistent with a free-radical mechanism for the decomposition of pyrimidine.

A free-radical mechanism is also supported by evidence of chain carriers, and of radical termination products present as products of reaction. The large concentrations of H_2 observed in the reaction products would be formed if H atoms were radical chain carriers. CN radicals are evident from the detection of cyanogen, which could be formed from either a termination reaction, or by the reaction of a CN radical with HCN[14] or a nitrile product of reaction.[15] Either of the chain carriers would be expected to propagate through H-abstraction from pyrimidine to yield *o*-, *p*- or 5-pyrimidyl radicals (see Table 2 for structures of the pyrimidyl radicals).

The most likely initiation process in the free-radical decomposition of pyrimidine would take place through C—H bond fission to yield a pyrimidyl radical. If the C—H bond energy in pyrimidine is assumed to be the same as that for the C—H bond in the *o*-position of pyridine[1,3,18] (*i.e.* 420 kJ mol^{-1}), an activation energy of *ca.* 420 kJ mol^{-1} is obtained. This is considerably higher than the activation energy of 275 (±13) kJ mol^{-1} observed for the decomposition of pyrimidine.

The relatively low overall activation energy observed for the decomposition of pyrimidine suggests that the rate of decomposition is strongly influenced by the rate of propagation steps of the free-radical chain mechanism. In the case of pyridine,[1,18] the overall rate of disappearance of reactant corresponds to the rate of the initiation reaction yielding *o*-pyridyl and H radicals. It is an interesting question as to why the kinetics of reaction for the two systems would be so different, when the rates of the initiation reactions would be expected to be similar. Explanations for the difference in the overall kinetics between pyridine and pyrimidine can only be made with some knowledge of the mechanism for decomposition of pyrimidine. In the discussion to follow, a free-radical mechanism for the decomposition of pyrimidine will be postulated. Using kinetic modelling, the validity of the reaction mechanism will be tested to ensure that the temperature profiles of the major products predicted by the mechanism agree with the observed profiles.

Table 2 Thermochemical parameters for the pyrimidine system

structure	name[a]	$\Delta_f H^\circ_{300}$/ kJ mol^{-1}	S°_{300}/ J mol^{-1} K^{-1}
	PMD	193[b]	282[c]
	*p*-PMDYL	405	290
	*o*-PMDYL[d]	376	287
	5-pyrimidyl[e]	440	—
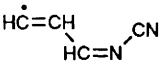	C_3H_3NCN[f]	520	350
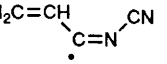	$BC_3H_4N_2$[d,f]	500	350
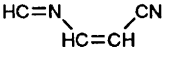	NC_3H_3CN	520	350
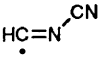	HCNCN[d,f]	450	290

[a] Name as shown in Table 3. [b] Ref. 16. [c] Calculated from data in review article ref. 17. [d] Heat of formation optimised using kinetic modelling. [e] Not included in kinetic model (see text). [f] Calculated assuming $N_f(CN) = C_D(H)(CN) - C_D(H)(C) + N_f(C)$.

Reaction Mechanism

The pyrimidyl radicals would be expected to be important radicals in the decomposition mechanism of pyrimidine. They would be formed in initiation reactions yielding pyrimidyl and H atoms, and from the abstraction of H from pyrimidine by H atoms or CN radicals to yield pyrimidyl and H_2 or HCN. The relative importance of the three pyrimidyl radicals would be largely determined from their thermochemistry, and also from the rate at which the particular pyrimidyl radical can decompose to form stable products and regenerate the chain carriers H and CN. If there is no low-energy pathway for the decomposition of a pyrimidyl radical, it will tend to recombine with H atoms to reform pyrimidine.

Some insight into the relative stability of the pyrimidyl radicals can be gleaned from studies on the decomposition of pyridine.[1,18] The heat of formation of *o*-pyridyl derived from these earlier studies suggests that the radical centre interacts with the nitrogen lone pair in the case of *o*-pyridyl. This

results in *o*-pyridyl being *ca.* 35 kJ mol^{-1} more stable[1] than predicted by assuming the *o*-C—H bond strength in pyridine to be the same as the C—H bond strength in benzene. This conclusion is supported by *ab initio* molecular orbital calculations[19] on *o*-pyridyl. These calculations indicated that there is significant interaction between the radical centre and the nitrogen lone pair in *o*-pyridyl.

Estimation of the heats of formation of the pyrimidyl radicals is complicated by the possibility of the radical centre being *ortho* to no nitrogen atoms (the 5-pyrimidyl radical), one nitrogen atom (the *p*-pyrimidyl radical), or two nitrogen atoms (the *o*-pyrimidyl radical). The heat of formation of the 5-pyrimidyl radical should be estimable from the C—H bond strength of benzene, yielding a heat of formation (at 300 K) of 440 kJ mol^{-1}. It would be anticipated that for the pyrimidyl radical, where the radical centre is *ortho* to a single N atom, the heat of formation should be estimable from the *o*-C—H bond strength in pyridine. This yields a heat of formation of 405 kJ mol^{-1}.

The heat of formation of the *o*-pyrimidyl radical is difficult to estimate since there is no previously studied radical which would be a useful analogue for this species. However, it would be logical to expect that the stabilisation of *o*-pyrimidyl would be no less than that observed for *o*-pyridyl. An upper limit for the stabilisation energy in *o*-pyrimidyl could be taken to be double the stabilisation energy of *o*-pyridyl. Using this upper and lower limit, the heat of formation of *o*-pyrimidyl would be expected to fall within the range 370–405 kJ mol^{-1}. Refinement of this estimate will be discussed later, when the results of the kinetic modelling of the decomposition of pyrimidine are presented.

On the basis of the estimated relative heats of formation of the pyrimidyl radicals, it is not possible to exclude the 5-pyrimidyl radical from being important in the decomposition mechanism for pyrimidine. The expected high heat of formation of this species makes it unlikely to be formed in an important initiation pathway, however. Its estimated heat of formation would also suggest that its formation by H-abstraction by H atoms would be endothermic by *ca.* 20 kJ mol^{-1}. Nevertheless, because of the high heat of formation of the CN radical, abstraction of H from pyrimidine by CN to form the 5-radical would be exothermic. Therefore on the basis of thermochemistry alone, the 5-pyrimidyl radical cannot be excluded from playing a role in the decomposition of pyrimidine.

Using the group additivity method outlined by Benson,[20] the energetics of various pathways to products from the pyrimidyls have been explored. Both the *o*- and the *p*-pyrimidyl radical can undergo simple ring fission to yield cyano radicals. The *p*-pyrimidyl radical can also undergo fission to yield an acetylenic open-chain radical which is estimated to have a heat of formation 160 kJ mol^{-1} higher than that of the cyano radical. Ring fission to yield the cyano radical would therefore be greatly favoured. Similar conclusions have been made previously concerning the stability of open chain radicals in the pyridine system.[1]

The 5-pyrimidyl radical differs from the other pyrimidyls in that it cannot undergo fission to yield a cyano-radical. It is therefore unlikely that the 5-pyrimidyl radical could undergo decomposition to yield products. On this basis the 5-pyrimidyl radical can be considered to be a species of little importance in the decomposition of pyrimidine.

The decomposition of the open-chain radicals formed from the fission of *o*- and *p*-pyrimidyls can be shown to lead to the observed products of pyrimidine decomposition. Importantly, these decomposition pathways also lead to the regeneration of the H atom or CN radical chain carriers.

In Scheme 1, pathways for the decomposition of the *para*-radical are illustrated. The heats of formation of the various intermediates as estimated by group additivity are given in Table 2. It can be seen that *p*-pyrimidyl decomposes to form HCN and cyanovinyl radical. Cyanovinyl would principally undergo loss of an H atom to form cyanoacetylene, although H abstraction from pyrimidine by cyanovinyl could also be a minor route for the formation of acrylonitrile.

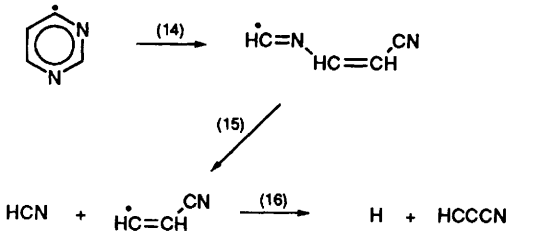

Scheme 1 Reaction scheme for decomposition of the *p*-pyrimidyl radical. Numbers in brackets refer to reaction number in Table 3.

The decomposition routes of the *o*-pyrimidyl radical are shown in Scheme 2. There are two thermochemically feasible pathways by which *o*-pyrimidyl can decompose. Through a series of simple fission steps, acetylene and HCN are the stable products formed, with CN radical being regenerated. Alternatively, the radical formed from the ring opening reaction of *o*-pyrimidyl could undergo 1,3-H transfer to yield a species which cleaves to form CN radicals and acrylonitrile. It should be noted that unlike *p*-pyrimidyl, the CN radical is regenerated in the decomposition of *o*-pyrimidyl, in both of the possible pathways.

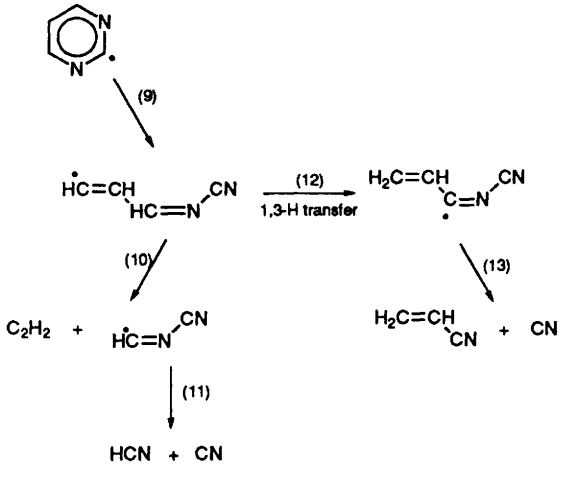

Scheme 2 Reaction scheme for decomposition of the *o*-pyrimidyl radical. Numbers in brackets refer to reaction number in Table 3.

In the development of a kinetic model, rate constants must be estimated in addition to the thermochemistry of the participating species. Rate constants for the reactions illustrated in Schemes 1 and 2 have been estimated largely by analogy to previously studied systems. The relationship between the activation energy and the enthalpy change for various types of reaction has been discussed by Benson.[20] The range of possible Arrhenius pre-exponential factors for the reaction types has also been discussed by Benson.[20]

By means of kinetic modelling these initial estimates of the Arrhenius parameters for the various reactions can be refined. Through the use of sensitivity and flux analysis, the effects of these parameters on the predictions of the model can be assessed.

Kinetic Modelling

Kinetic modelling was carried out using the CHEMKIN[21] code, in addition to a shock tube code[22] and the ordinary differential equation solver LSODE.[23] The shock tube code

Table 3 Reaction model for pyrimidine pyrolysis[a]

	forward reaction			reverse reaction			
reactions	log A	n	E	log A	n	E	ref.
1 *o*-PMDYL + H ⇌ PMD	13.56	0.00	0.0	15.09	0.00	397.8	S
2 *p*-PMDYL + H ⇌ PMD	13.58	0.00	0.0	15.42	0.00	427.1	est
3 H + PMD ⇌ *o*-PMDYL + H_2	12.70	0.00	33.4	11.77	0.00	72.2	S
4 CN + PMD ⇌ HCN + *o*-PMDYL	13.30	0.00	25.1	12.89	0.00	139.6	S
5 HCCHCN + PMD ⇌ H_2CCHCN + *o*-PMDYL	11.30	0.00	41.8	11.64	0.00	86.2	est
6 H + PMD ⇌ *p*-PMDYL + H_2	12.78	0.00	41.8	11.55	0.00	51.3	S
7 CN + PMD ⇌ *p*-PMDYL + HCN	13.30	0.00	37.6	12.58	0.00	122.9	S
8 HCCHCN + PMD ⇌ *p*-PMDYL + H_2CCHCN	11.48	0.00	46.0	11.51	0.00	61.2	est
9 C_3H_3NCN ⇌ *o*-PMDYL	11.00	0.00	20.9	15.08	0.00	175.2	est
10 C_2H_2 + HCNCN ⇌ C_3H_3NCN	12.48	0.00	16.7	14.43	0.00	151.0	S
11 CN + HCN ⇌ HCNCN	13.00	0.00	8.4	13.10	0.00	115.8	S
12 C_3H_3NCN ⇌ $BC_4H_3N_2$	12.85	0.00	102.4	12.84	0.00	123.3	S
13 H_2CCHCN + CN ⇌ $BC_4H_3N_2$	13.60	0.00	20.9	13.99	0.00	114.8	est
14 *p*-PMDYL ⇌ NC_3H_3CN	14.90	0.00	154.7	11.13	0.00	29.7	est
15 NC_3H_3CN ⇌ HCN + HCCHCN	14.00	0.00	41.8	12.86	0.00	38.9	est
16 HCCHCN + M ⇌ HC_3N + H + M	15.90	0.00	179.7	16.67	0.00	16.8	1
17 H + HCCHCN ⇌ H_2CCHCN	13.30	0.00	0.0	15.18	0.00	442.2	est
18 H + H_2CCHCN ⇌ C_2H_3 + HCN	13.00	0.00	29.3	11.06	0.00	29.3	S
19 H + H_2CCHCN ⇌ H_2 + HCCHCN	13.00	0.00	33.4	11.73	0.00	27.8	est
20 H + C_2H_2(+M) ⇌ C_2H_3(+M)	13.00	0.00	11.3	12.73	0.00	180.1	25
21 2H + M ⇌ H_2 + M	18.00	−1.00	0.0	15.04	0.00	425.0	26
22 CN + HCN ⇌ C_2N_2 + H	7.58	1.57	0.4	14.60	0.00	47.0	14
23 CN + H_2 ⇌ HCN + H	5.69	2.44	8.9	14.94	0.00	112.8	27
24 C_2N_2 + M ⇌ 2CN + M	16.86	0.00	419.7	14.32	0.00	−121.1	28
25 HCN + M ⇌ H + CN + M	15.66	0.00	440.2	14.54	0.00	−72.1	29

[a] Units for A are $cm^3\ mol^{-1}\ s^{-1}$ or s^{-1} as appropriate. Units for E are $kJ\ mol^{-1}$. S indicates rate constant to which the model predictions are sensitive, est indicates rate constant estimate to which model predictions are not sensitive.

was modified to take into account cooling by the reflected rarefaction wave and to allow for reaction to occur in the cooling wave.

A detailed kinetic model for the pyrolysis of pyrimidine is included in Table 3. The model consists of pathways illustrated in Schemes 1 and 2, in addition to radical–radical and radical abstraction reactions not shown in the schemes. An explanation of the symbols used in Table 3 is given in Table 2.

Product and reactant concentration profiles predicted by the model are compared with experiment in Fig. 1–5. It can be seen that the model predictions are in good agreement with the experimental data. At low to moderate extents of decomposition, the model predictions are very sensitive to the estimated rates of reactions included in the model. The methods for estimation of the reaction rates, discussed above, result in rates which are strongly dependent on the proposed reaction pathway. Therefore the ability of the model to predict the reactant and product profiles at low to intermediate extents of decomposition strongly supports the proposed mechanism.

Included in Fig. 1–5 are model predictions for the low-concentration series of experiments. These predictions test whether the model is able to reproduce the observed order of the reaction. The model predicts an order of reaction of slightly greater than first order, with respect to reactant, for the rate of disappearance of reactant and the rate of formation of products. This slightly non-first-order behaviour predicted by the model is observed experimentally only for cyanoacetylene, acrylonitrile and acetylene. The model predicts the formation of HCN to be slightly greater than first order, which is not observed experimentally. When comparing the model predictions for the low-concentration runs with the experimental data, the lower accuracy of the low concentration data must be considered. Difficulties in measuring low levels of HCN could easily account for the deviations of the model predictions from the experimental measurements.

It was previously concluded on the basis of the experimental data that the decomposition of pyrimidine proceeds at a rate which is close to first order with respect to the reactant concentration. The low-concentration series of experiments uses reactant concentrations which are a factor of approximately four lower than the high concentration series. The model, however, predicts only small changes in the rate of formation of products and disappearance of reactant for the two reactant concentrations studied. The model therefore supports the conclusion based on the experimental observations that the rate of pyrimidine decomposition is close to first order with respect to reactant concentration. The model, however, predicts the order of the reaction to be slightly greater than 1. Considering the difficulty in measuring the products for the low-concentration series, this conclusion based on the modelling may indicate that the order of the reaction is non-integer, which is common for free-radical chain mechanisms of long kinetic chain length.

Optimisation of the rate of the initiation reaction to yield *o*-pyrimidyl and H-atoms has allowed the initial estimate of the heat of formation of *o*-pyrimidyl to be refined. The final value for the heat of formation of *o*-pyrimidyl was found to be 376 (±10) $kJ\ mol^{-1}$. This falls within the earlier estimated upper and lower limits, based on the heat of formation of *o*-pyridyl.

Sensitivity and Flux Analysis

When interpreting the results of sensitivity analysis it should be remembered that these are calculations based on the given kinetic model. Their relevance to the decomposition of pyrimidine will depend therefore on the correctness of the model.

Fig. 9–11 show variation in the sensitivity coefficients with temperature for the most sensitive reactions for formation of HCN, cyanoacetylene and acrylonitrile. The reactions important for the formation of these products are also important

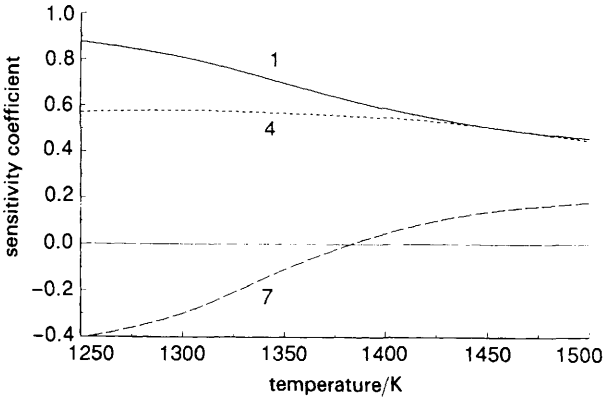

Fig. 9 Variation with temperature of the sensitivity coefficients for HCN. Only the most sensitive reactions from Table 3 are shown. Numbers refer to reaction number in Table 3.

for the formation of acetylene, and for the rate of decomposition of the reactant.

From the sensitivity plots for HCN and acrylonitrile, competition between the decomposition pathways involving *o*-pyrimidyl and *p*-pyrimidyl is evident. This is manifested in the form of negative sensitivity coefficients for the rate of H-abstraction from pyrimidine by CN to yield *p*-pyrimidyl. The negative sensitivity coefficient has been shown by flux analysis not to be due to the reaction moving in the reverse direction. HCN and acrylonitrile are both formed from the

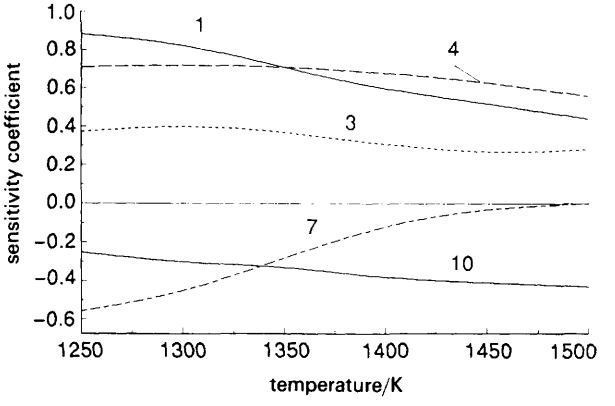

Fig. 10 Variation with temperature of the sensitivity coefficients for acrylonitrile. Only the most sensitive reactions from Table 3 are shown. Numbers refer to reaction number in Table 3.

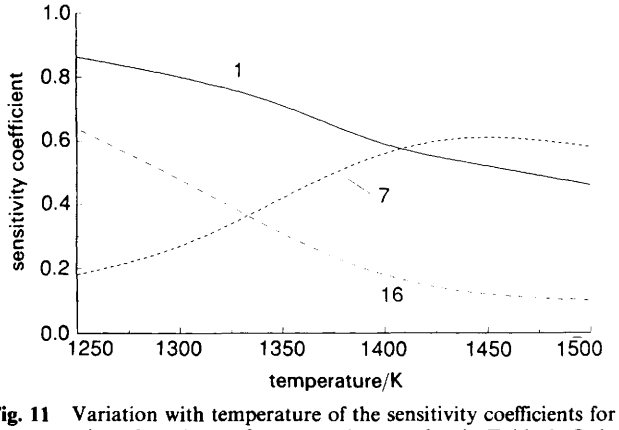

Fig. 11 Variation with temperature of the sensitivity coefficients for cyanoacetylene. Numbers refer to reaction number in Table 3. Only the most senstive reactions from Table 3 are shown.

o-pyrimidyl radical, meaning that any abstraction to yield the *p*-pyrimidyl radical will tend to decrease the quantity of these products formed.

The plots of sensitivity coefficients illustrate the rate-determining nature of the H-abstraction reaction by CN radicals. The rate of H abstraction by CN and the rate of the initiation reaction yielding *o*-pyrimidyl and H atoms have a comparable effect on the concentrations of HCN and acrylonitrile.

The importance of the rate of H-abstraction from pyrimidine by CN can help to explain the low apparent activation energy of the overall rate of disappearance of pyrimidine. Previous modelling studies on the decomposition of pyridine,[1] 2-picoline,[4] and the butenenitriles[24] have shown that for these systems the rates of formation of products are influenced mainly by the initiation reactions. In each of these cases the overall rate of decomposition of the reactant closely corresponded to the rate of the initiation reaction of the free-radical decomposition mechanism. This is typical of kinetic data obtained for pyrolysis reactions using the shock tube, and is a consequence of the short residence time of this type of experiment. The observation of an overall rate of disappearance of reactant being close to the initiation rate for the decomposition mechanism is in contrast to the observed rate parameters for pyrimidine pyrolysis. In the case of pyrimidine, sensitivities to the rate constant for H-abstraction of pyrimidine by CN show comparable sensitivity to the initiation reactions over the entire range of temperatures studied, and thus a relatively low overall activation energy is observed.

The concept of 'kinetic chain length' described by Benson[20] can be used to rationalise the differences in the kinetics of pyrimidine and pyridine. In the case of pyridine, since the rate of the initiation step is close to the overall rate of pyridine decomposition, the kinetic chain length is *ca.* 1. This is very different from the pyrimidine case in which the rate of decomposition is much faster than the rate of initiation, yielding a chain length of *ca.* 80 at 1350 K. This illustrates the greater importance of propagation steps in the case of pyrimidine, and the low activation energy observed for overall kinetics reflects this importance.

Having established that the low activation energy for the decomposition of pyrimidine is a result of increased influence of propagation steps, it is interesting to try to draw conclusions about which aspects of the pyrimidine pyrolysis mechanism give rise to this behaviour. The CN radical is an important propagating radical in the decomposition of pyrimidine, with the major products HCN and acrylonitrile being formed from CN chains. This is a major difference between the mechanism for pyrimidine decomposition, and the mechanism of decomposition of the other organonitrogen compounds studied.[1,2,4,24] For pyridine, at low to moderate extents of decomposition, the radical chain carriers are H-atoms. The radical chain carriers for the butenenitriles and 2-picoline are H-atoms and methyl radicals. It is possible that CN chains propagate much more rapidly than H or methyl chains with less efficient termination reactions. This would result in the large kinetic chain length observed for pyrimidine.

The importance of CN radicals in the decomposition of pyrimidine can be attributed to the high heat of formation of pyrimidine compared with pyridine or 2-picoline. The open-chain C_3H_3NCN radical, formed from *o*-pyrimidyl, can undergo decomposition in two steps to yield acetylene, HCN and CN. The total endotherm for the formation of these products from the open-chain radical is 280 kJ mol^{-1}. In the case of pyridine, the open-chain C_4H_4CN radical formed from the ring opening of *o*-pyridyl[1] could decompose in an

analogous fashion to yield two acetylene molecules and CN. However, the total endotherm for the formation of these products from the open-chain C_4H_4CN radical is 410 kJ mol^{-1}. The considerably higher endotherm for generation of the CN radical in the pyridine system explains why CN radicals are of little importance in the pyrolysis of pyridine at low to intermediate extents of decomposition.

Conclusion

Thermal decomposition of pyrimidine dilute in argon takes place over the temperature range 1200–1600 K, at a residence time of 850 to 1000 μs, and pressure of 13–15 atm. A free-radical mechanism consisting of 25 reactions has been shown to predict successfully the concentrations of products formed and of pyrimidine remaining in the product mixtures. Important radicals in this mechanism are *o*- and *p*-pyrimidyl, with H atoms and CN radicals being the radical chain carriers. The CN radical as a chain carrier in the decomposition of pyrimidine is a significant departure from the decomposition mechanisms of other organo-nitrogen compounds such as 2-picoline, pyridine or pyrrole. It is postulated that the relatively low overall activation energy for the rate of decomposition of pyrimidine is due to the efficiency of the CN chain. The feasibility of generation of CN from intermediate radicals in the decomposition of pyrimidine is thought to be a consequence of the relatively high heat of formation of pyrimidine.

The authors thank Jacqueline Palmer for assistance with the SPST experiments. The financial assistance of the Australian Research Council is gratefully acknowledged.

References

1 J. C. Mackie, M. B. Colket and P. F. Nelson, *J. Phys. Chem.*, 1990, **94**, 4099.
2 J. C. Mackie, M. B. Colket, P. F. Nelson and M. Esler, *Int. J. Chem. Kinet.*, 1991, **23**, 733.
3 A. Terentis, A. Doughty and J. C. Mackie, *J. Phys. Chem.*, 1992, **96**, 10334.
4 A. Doughty and J. C. Mackie, *J. Phys. Chem.*, 1992, **96**, 10339.
5 L. R. Snyder, *Anal. Chem.*, 1969, **41**, 314.
6 D. T. Clarke and R. Wilson, *Fuel*, 1983, **62**, 1034.
7 S. Wallace, K. D. Bartle and D. L. Perry, *Fuel*, 1989, **68**, 1450.
8 P. F. Nelson, A. N. Buckley and M. D. Kelly, *24th International Symposium on Combustion*, The Combustion Institute, Sydney, 1992, p. 1259.
9 R. D. Hauck, *ACS Fuel Chem.*, 1975, **20**, 85.
10 S. R. Palmer, E. J. Hippo, M. A. Kruge and J. C. Crelling, *Proceedings of the International Conference on Coal Science*, Butterworth–Heinemann, Oxford, 1991, p. 993.
11 W. S. Cathro and J. C. Mackie, *J. Chem. Soc., Faraday Trans.*, 1972, **68**, 150.
12 K. R. Doolan and J. C. Mackie, *Combust. Flame* 1983, **49**, 221.
13 K. K. Innes, H. D. McSwiney Jr., J. D. Simmons and S. G. Tilford, *J. Mol. Spectrosc.*, 1969, **31**, 76.
14 A. Szekely, R. K. Hanson and C. T. Bowman, *Int. J. Chem. Kinet.*, 1983, **15**, 1237.
15 S. Zabarnick and M. C. Lin, *Chem. Phys.*, 1989, **134**, 185.
16 M. Nabavian, R. Sabbah, R. Chastel and M. Laffitte, *J. Chim. Phys.*, 1977, **74**, 115.
17 K. K. Innes, I. G. Ross and W. R. Williams, *J. Mol. Spectrosc.*, 1988, **132**, 492.
18 H. I. Leidreiter and H. G. Wagner, *Z. Phys. Chem., Neue Folge*, 1987, **153**, 99.
19 O. Kikuchi, Y. Hondo, K. Morihashi and M. Nakayama, *M. Bull. Chem.*, 1988, **61**, 291.
20 S. W. Benson, *Thermochemical Kinetics*, Wiley, New York, 1976.
21 R. J. Kee, J. A. Millar and T. H. Jefferson, CHEMKIN; A General Purpose, Problem Independent, Transportable FORTRAN Chemical Kinetics Codes Package, Sandia National Laboratories Report SAN80-003, March, 1980.
22 R. E. Mitchell and R. J. Kee, A General Purpose Kinetic Code for Predicting Chemical Kinetic Behaviour Behind Incident and Reflected Shocks. Sandia National Laboratories, SAN82-8205, March, 1982.
23 A. C. Hindmarsh, LSODE and LSODE; Two New Initial Value Differential Equation Solvers, *ACM Signum Newsletters*, 1980, **15**.
24 A. Doughty and J. C. Mackie, *J. Phys. Chem.*, 1992, **96**, 272.
25 W. A. Payne and L. J. Stief, *J. Chem. Phys.*, 1976, **64**, 1150.
26 G. Dixon-Lewis, *Philos. Trans. R. Soc. London, Ser. A*, 1981, **A303**, 181.
27 B. Atakan, A. Jacobs, M. Wahl, R. Weller and J. Wolfrum, *Chem. Phys. Lett.*, 1989, **154**, 449.
28 A. Szekely, R. K. Hanson and C. T. Bowman, *J. Chem. Phys.*, 1984, **80**, 4982; M. B. Colket, *Int. J. Chem. Kinet.*, 1984, **16**, 353; T. Fueno, K. Tabayashi and O. Kajimoto, *J. Phys. Chem.*, 1973, **77**, 575; K. Najarajan, K. Thielen, H. D. Hermanns and P. Roth, *Ber. Bunsenges. Phys. Chem.*, 1986, **90**, 533; M. W. Slack, E. S. Fishburne and A. R. Johnson, *J. Chem. Phys.*, 1971, **54**, 1652.
29 P. Roth and Th. Just, *Ber. Bunsenges. Phys. Chem.*, 1976, **80**, 171; P. Roth, *Forsh. Ingenieurwes*, 1980, **46**, 93; A. Szekely, R. K. Hanson and C. T. Bowman, *Symp. Int. Shock Tubes Waves Proc.*, 1982, **13**, 617; A. Szekely, R. K. Hanson and C. T. Bowman, *J. Phys. Chem.*, 1984, **88**, 666; P. Roth and Th. Just, *Materials Research Symp. Proc., NBS Spec. Pub. 561*, 1979, **10**, 91; K. Thielen and P. Roth, *Combust. Flame*, 1987, **69**, 141.

Paper 3/04723G; *Received 5th August*, 1993